Proceedings of the ASME 2009 3rd International Conference of Energy Sustainability
ES2009
July 19-23, 2009, San Francisco, California, USA

ES2009-90441

HAWT Rotor Design and Performance Analysis

Emrah Kulunk[a] and Nadir Yilmaz[b]
[a] New Mexico Institute of Mining and Technology, Socorro, USA, E-mail: ekulunk@nmt.edu
[b] New Mexico Institute of Mining and Technology, Socorro, USA, E-mail: nadir@nmt.edu

Abstract

In this paper, a design method based on blade element momentum (BEM) theory is explained for horizontal-axis wind turbine (HAWT) blades. The method is used to optimize the chord and twist distributions of the blades. Applying this method a 100kW HAWT rotor is designed. Also a computer program is written to estimate the aerodynamic performance of the existing HAWT blades and used for the performance analysis of the designed 100kW HAWT rotor.

Keywords: HAWT Design, Blade Element Momentum Theory, Wind Energy, Aerodynamics

Nomenclature

C_P: Power coefficient of wind turbine rotor
C_T: Thrust coefficient of wind turbine rotor
C_{T_r} : Local thrust coef. of each annular rotor section
P: Power output from wind turbine rotor
$\dot{m}$: Air mass flow rate through rotor plane
U_∞: Free stream velocity of wind
U_{rel}: Relative wind velocity
U_R: Uniform wind velocity at rotor plane
A : Area of wind turbine rotor
R : Radius of wind turbine rotor
r : Radial coordinate at rotor plane
r_i : Blade radius for the ith blade element
p' : Pressure drop across rotor plane
H: Bernoulli's constant
T : rotor thrust
Q : rotor torque
F_D: Drag force on an annular blade element
F_L: Lift force on an annular blade element
C_D: Drag coefficient of an airfoil
C_L: Lift coefficient of an airfoil
f : Tip-loss factor
f_i: Tip-loss factor for the ith blade element
N : Number of blade elements
B : Number of blades of a rotor
a : Axial induction factor at rotor plane
a' : Angular induction factor
λ : Tip-speed ratio of rotor
λ_d: Design tip-speed ratio
λ_r: Local tip-speed ratio
$\lambda_{r,i}$: Local tip-speed ratio for the ith blade element
c_i:: Blade chord length for the ith blade element
ρ : Air density
Ω : Angular velocity of wind turbine rotor
α : Angle of attack
θ_i: Pitch angle for the ith blade element
$\varphi_{opt,i}$: Optimum relative wind angle for the ith blade element
σ: Solidity ratio
ν: Kinematic viscosity of air
γ: Glide ratio
Re: Reynolds number
HAWT: Horizontal-axis wind turbine
BEM: Blade element momentum

1. Introduction

The objectives of this study are to develop a method using BEM theory for aerodynamic design of the HAWT blades and performance analysis of the existing blades, also to build a computer program using this method and to design a 100kW HAWT rotor performing the program, finally to determine the aerodynamic characteristics and to create the performance curves of the designed rotor.

The scope of the study is restricted to aerodynamics of HAWTs, blade design procedure for an optimum rotor using BEM theory and performance analysis of the designed rotor.

2. Aerodynamics of HAWTs

In order to develop a method for HAWT blade design, the general aerodynamic concepts of the HAWTs need to be introduced.

HAWT power production depends on the interaction between the rotor and the wind. So the major aspects of wind turbine performance like power output and loads are determined by the aerodynamic forces generated by the wind. These can only be understood with a deep comprehension of the aerodynamics of steady state operation.

The BEM theory combines two methods to analyze the aerodynamic performance of a wind turbine. These are momentum theory and blade-element theory which are used to outline the governing equations for the aerodynamic design and power prediction of a wind turbine rotor. Momentum theory examines the momentum balance on a rotating annular stream tube passing through a turbine and blade-element theory examines the forces generated by the aerofoil lift and drag coefficients at various sections along the blade. Combining these theories gives a series of equations that can be solved iteratively.

The analysis of the aerodynamic behavior of wind turbines can be started without any specific turbine design just by considering the energy extraction process. A simple model, known as actuator disc

model, can be used to determine the power from an ideal turbine rotor and the thrust of the wind on the ideal rotor (Figure 1). But this model is based on some assumptions like no frictional drag, homogenous, incompressible, steady state fluid flow, constant pressure increment or thrust per unit area over the disk, continuity of velocity through the disk and an infinite number of blades.

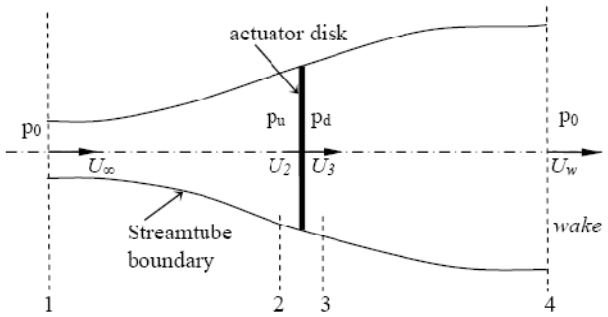

Figure 1. Actuator Disk

The analysis of the actuator disk theory assumes a control volume, in which the control volume boundaries are the surface of a stream tube and two cross-sections of the stream tube. In order to analyze this control volume, four stations (1: free-stream region, 2: just before the blades, 3: just after the blades, 4: far wake region) need to be considered (Figure 1).

The mass flow rate must be the same everywhere along the stream tube.

$$\rho A_\infty U_\infty = \rho A_d U_d = \rho A_w U_w \tag{1}$$

Assuming the continuity of velocity through the disk gives

$$\mathrm{U_2 = U_3 = U_R} \tag{2}$$

For steady state flow the mass flow rate is

$$\dot{m} = \rho A U_R \tag{3}$$

Applying the conservation of linear momentum

$$T = \dot{m}(U_\infty - U_w) \tag{4}$$

can be obtained. Since the flow is frictionless and no work is done on both sides of the rotor Bernoulli equation can be applied between station 1 and 2, then 3 and 4.

$$p_d + \frac{1}{2}\rho U_R^2 = p_o + \frac{1}{2}\rho U_w^2 \tag{5}$$

$$p_o + \frac{1}{2}\rho U_\infty^2 = p_u + \frac{1}{2}\rho U_R^2 \tag{6}$$

Using equations 5 and 6, the pressure decrease, *p′* can be found as

$$p' = \frac{1}{2}\rho(U_\infty^2 - U_w^2) \tag{7}$$

Also the thrust can be expressed as the sum of the forces on each side

$$T = Ap' \tag{8}$$

where

$$p' = (p_u - p_d) \tag{9}$$

Substituting equation 7 into equation 8 gives

$$T = \frac{1}{2}A\rho(U_\infty^2 - U_w^2) \tag{10}$$

Using the equations 3, 4, and 10

$$U_R = \frac{U_\infty + U_w}{2} \tag{11}$$

can be obtained and defining the axial induction factor α as

$$a = \frac{U_\infty - U_R}{U_\infty} \tag{12}$$

gives

$$U_R = U_\infty(1 - a) \tag{13}$$

$$U_w = U_\infty(1 - 2a) \tag{14}$$

To find the power output of the rotor

$$P = TU_R \tag{15}$$

can be used. By substituting equation 10 into 15

$$P = \frac{1}{2}\rho(U_\infty^2 - U_w^2)U_R \tag{16}$$

can be written. Also substituting equations 13 and 14 into equation 15 gives

$$P = 2\rho A a U_\infty^3(1 - a)^2 \tag{17}$$

The performance parameters of a HAWT rotor (power coefficient, C_P thrust coefficient, C_T and the tip-speed ratio, λ) can be expressed in dimensionless form which is given in equation 18, 19 and 20 respectively.

$$C_P = \frac{2P}{\rho U_\infty^3 \pi R^2} \tag{18}$$

$$C_T = \frac{2T}{\rho U_\infty^2 \pi R^2} \tag{19}$$

$$\lambda = \frac{R\Omega}{U_\infty} \tag{20}$$

Substituting equation 17 into equation 18 gives

$$C_P = 4a(1-a)^2 \tag{21}$$

Using the equations 10, 13 and 17 the axial thrust on the disk can be rewritten as

$$T = 2Aa\rho(1-a)U_\infty^2 \tag{22}$$

Finally substituting equation 22 into equation 19 gives

$$C_T = 4a(1-a) \tag{23}$$

Thus far the method is developed on the assumption that there was no rotational motion. To extend the method developed, the effects of this rotational motion needs to be included so it is necessary to modify the qualities of the actuator disk by assuming that it can also impart a rotational component to the fluid velocity while the axial and radial components remain unchanged. Using a rotating annular stream tube analysis, equations can be written that express the relation between the wake velocities (both axial and rotational) and the corresponding wind velocities at the rotor disk.

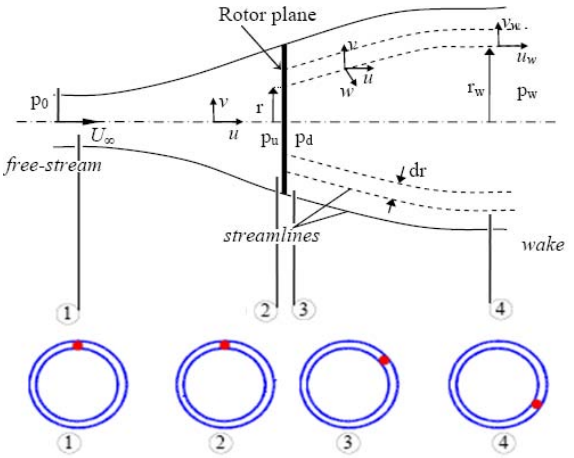

Figure 2. Rotating Annular Stream Tube Analysis

This analysis considers the conservation of angular momentum in the annular stream tube (Figure 2). If the condition of continuity of flow is applied for the annular element

$$u_w r_w dr_w = urdr \tag{24}$$

can be obtained. Conservation of the angular momentum of the fluid gives

$$w_w r_w^2 = wr^2 \tag{25}$$

Also

$$dQ = \rho uwr^2 dA \tag{26}$$

which can be written for the radial blade element, where $dA = 2r\pi dr$. Applying the Bernoulli equation between station 1 and 2 then between 3 and 4 gives

$$H_o = p_o + \frac{1}{2}\rho U_\infty^2 = p_u + \frac{1}{2}\rho(u^2+v^2)$$

$$H_1 = p_d + \frac{1}{2}\rho(u^2+v^2+w^2r^2) = p_w + \frac{1}{2}\rho(u_w^2 + r_w^2 w_w^2)$$

And taking the difference between H_0 and H_1 gives

$$H_o - H_1 = p' - \frac{1}{2}\rho(w^2r^2)$$

Which means the kinetic energy of the rotational motion given to the fluid by the torque of the blade is equal to $-(1/2)\rho(w^2r^2)$. The total pressure head is

$$\begin{aligned} p_o - p_w &= \frac{1}{2}\rho(u_w^2 - U_\infty^2) + \frac{1}{2}w_w^2\rho r_w^2 \\ &\quad + (H_o - H_1) \\ &= \frac{1}{2}\rho(u_w^2 - U_\infty^2) + \frac{1}{2}\rho(w_w^2 r_w^2 \\ &\quad - w^2r^2) + p' \end{aligned} \tag{27}$$

Applying the Bernoulli's equation between station 2 and 3 gives the pressure drop, p'

$$p' = \frac{1}{2}\rho[-\Omega^2 + (\Omega+w)^2]r^2 = \rho\left(\Omega + \frac{w}{2}\right)wr^2 \tag{28}$$

Substituting this result into the equation 27 gives

$$p_o - p_w = \frac{1}{2}\rho(u_w^2 - U_\infty^2) + \rho\left(\Omega + \frac{w}{2}\right)r_w^2 w_w \tag{29}$$

In station 4, the pressure gradient can be written as

$$\frac{dp_w}{dr_w} = \rho r_w w_w^2 \tag{30}$$

Differentiating equation 29 relative to r_w and equating to equation 30 gives

$$\frac{1}{2}\frac{d}{dr_w}(U_\infty^2 - u_w^2) = (\Omega + w_w)\frac{d}{dr_w}(r_w^2 w_w) \tag{31}$$

The equation of axial momentum for the blade element in differential form can be written as

$$dT = \rho u_w(U_\infty - u_w)dA_w + (p_o - p_w)dA_w \tag{32}$$

Since $dT = p'dA$,

$$dT = \rho\left(\Omega + \frac{w}{2}\right)wr^2 dA \tag{33}$$

can be written. Finally, combining the equations 24, 27, 32 and 33 gives

$$\frac{1}{2}(U_\infty - u_w)^2 = \left(\frac{\Omega + w_w/2}{u_w} - \frac{\Omega + w/2}{U_\infty}\right)u_w r_w^2 w_w \tag{34}$$

An exact solution of the stream-tube equations can be obtained when the flow in the slipstream is not rotational except along the axis which implies that the rotational momentum wr^2 has the same value for all radial elements. Defining the axial velocities as $u = U_\infty(1-a)$ and $u_w = U_\infty(1-b)$ gives

$$a = \frac{b}{2}\left[1 - \frac{(1-a)b^2}{4\lambda^2(b-a)}\right] \tag{35}$$

And the element of thrust is equal to

$$\begin{aligned} dT &= 2\rho u(u-U_\infty)dA \\ &= 4\pi\rho U_\infty^2 a(1-a)rdr \end{aligned} \tag{36}$$

Using the equation 28

$$\begin{aligned} dT &= p'dA \\ &- 2\pi\rho(\Omega + w/2)wr^3dr \end{aligned} \tag{37}$$

can be written. If the angular induction factor is defined as $a' = \frac{w}{2\Omega}$, dT becomes

$$dT = 4\pi\rho\Omega^2 a'(1+a')r^3dr \tag{38}$$

In order to obtain a relationship between axial induction factor and angular induction factor, equation 37 and 38 can be equated which gives

$$\frac{a(1-a)}{a'(1+a')} = \frac{\Omega^2 r^2}{U_\infty^2} = \lambda_r^2 \tag{39}$$

Using the equation 26 the element of torque can be obtained as

$$dQ = 4\pi\rho U_\infty \Omega a'(1-a)r^3dr \tag{40}$$

Since the power generated at each radial element is given by equation of $dP = \Omega dQ$, substituting equation 40 it can be rewritten as

$$dP = \frac{1}{2}\rho A U_\infty^3\left[\frac{8}{\lambda^2}a'(1-a)\lambda_r^3 d\lambda_r\right] \tag{41}$$

Also the power coefficient for each annular ring can be written as

$$dC_p = \frac{dP}{1/2\rho U_\infty^3 A} \tag{42}$$

Substituting equation 41 into the equation 42 and integrating from hub tip speed ratio to the tip speed ratio gives

$$C_p = \frac{8}{\lambda^2}\int_{\lambda_h}^{\lambda} a'(1-a)\lambda_r^3 d\lambda_r \tag{43}$$

By solving equation 39 for a' in terms of a

$$a' = -\frac{1}{2} + \frac{1}{2}\sqrt{1 + \frac{4}{\lambda_r^2}a(1-a)} \tag{44}$$

can be obtained. Solving the equations 43 and 44 together for the maximum possible power production gives

$$\lambda_r^2 = \frac{(1-a)(4a-1)^2}{(1-3a)} \tag{45}$$

and substituting equation 45 into 39 gives the a' for maximum power in each annular ring.

$$a' = (1-3a)/(4a-1) \tag{46}$$

Differentiating the equation 45 with respect to a, a relationship between *r*, $d\lambda$ and da can be obtained.

$$2\lambda_r d\lambda_r - \left[6(4a-1)(1-2a)^2/(1-3a)^2\right]da \tag{47}$$

Finally, substituting the equations 45, 46, 47 into the equation 43 gives

$$C_{p,\max} = \frac{24}{\lambda^2}\int_{a_1}^{a_2}\left[\frac{(1-a)(1-2a)(1-4a)}{(1-3a)}\right]^2 da \tag{48}$$

Where a_1 is the corresponding axial induction factor for $\lambda_r = \lambda_h$ and a_2 is the corresponding axial induction factor for $\lambda_r = \lambda$.

Until this point the momentum theory is tried to be explained for the design method but it does not consider the effect of rotor geometry characteristics like blade airfoil, chord and twist distributions. For this reason blade element theory needs to be added to the design method. In order to apply blade element analysis, it is assumed that the blade is divided into N sections. This analysis is based on some assumptions like no aerodynamic interactions between different blade elements and the forces on the blade elements are solely determined by the lift and drag coefficients.

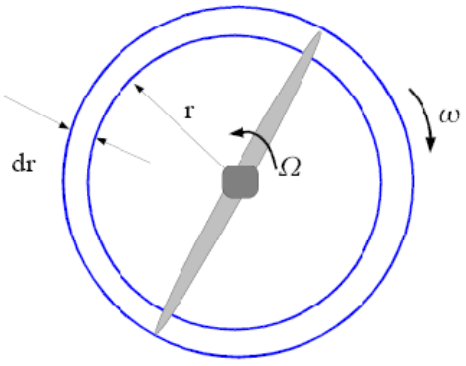

Figure 3. Rotating Annular Stream Tube

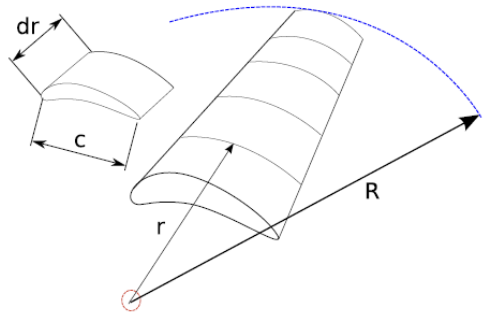

Figure 4. The Blade Element Model [1]

Since each of the blade elements has a different rotational speed and geometric characteristics they will experience a slightly different flow. So blade element theory involves dividing up the blade into a sufficient number (usually between ten and twenty) of elements and calculating the flow at each one. Overall performance characteristics of the blade are determined by numerical integration along the blade span (Figure 3, 4).

Lift and drag coefficient data are available for a variety of airfoils from wind tunnel data. Since most wind tunnel testing is done with the aerofoil stationary, the relative velocity over the airfoil is used in order to relate the flow over the moving airfoil with the stationary test (Figure 5).

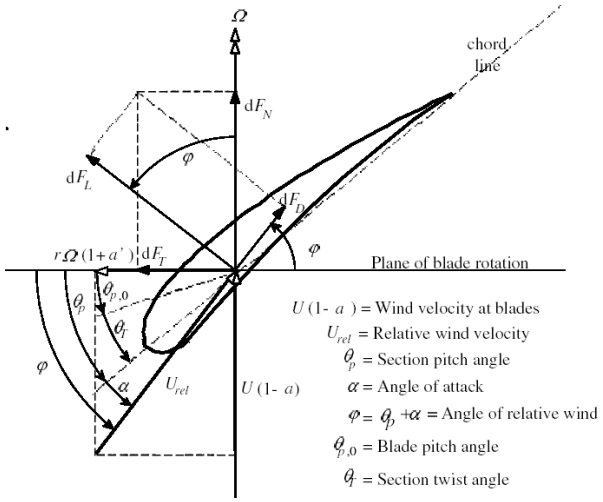

Figure 5. Blade Geometry for the analysis of a HAWT Rotor [6]

Examining Figure 5, the following equations can be immediately derived:

$$U_{rel} = \frac{U_\infty(1-a)}{\sin(\varphi)} \tag{49}$$

$$\tan(\varphi) = \frac{U_\infty(1-a)}{\Omega r(1+a')} = \frac{(1-a)}{(1+a')\lambda_r} \tag{50}$$

$$dF_L = C_L \frac{1}{2}\rho U_{rel}^2 c dr \tag{51}$$

$$dF_D = C_D \frac{1}{2}\rho U_{rel}^2 c dr \tag{52}$$

$$dL = dF_L \sin\varphi - dF_D \cos\varphi \tag{53}$$

$$dT = dF_L \cos\varphi + dF_D \sin\varphi \tag{54}$$

If the rotor has B number of blades, the equations 49, 51 and 52 can be rearranged.

$$dL = B\frac{1}{2}\rho U_{rel}^2 (C_L \sin\varphi - C_D \cos\varphi) c dr \tag{55}$$

$$dT = B\frac{1}{2}\rho U_{rel}^2 (C_L \cos\varphi + C_D \sin\varphi) c dr \tag{56}$$

The elemental torque can be written as $dQ = rdL$ which gives

$$dQ = B\frac{1}{2}\rho U_{rel}^2 (C_L \sin\varphi - C_D \cos\varphi) c r dr \tag{57}$$

Also examining Figure 5

$$U_{rel} = \frac{U_\infty(1-a)}{\sin\varphi} \tag{58}$$

can be derived. The solidity ratio can be defined as

$$\sigma = \frac{Bc}{2\pi r} \tag{59}$$

Finally, the general form of elemental torque and thrust equations becomes

$$dQ = \sigma\pi\rho \frac{U_\infty^2(1-a)^2}{\sin^2\varphi}(C_L \sin\varphi - C_D \cos\varphi) r^2 dr \tag{60}$$

$$dT = \sigma\pi\rho \frac{U_\infty^2(1-a)^2}{\sin^2\varphi}(C_L \cos\varphi - C_D \sin\varphi) r dr \tag{61}$$

Equations 60 and 61 define the normal force (thrust) and the tangential force (torque) on annular rotor section.

As it is stated before BEM theory refers to the determination of a wind turbine blade performance by combining the equations of general momentum theory and blade element theory, so equations 36 and 61 can be equated to obtain the following equation.

$$\frac{a}{(1-a)} = (\sigma C_L)\frac{\cos\varphi}{4\sin^2\varphi}\left[1+(C_D/C_L)\tan\varphi\right] \tag{62}$$

Also equating the equations 40 and 60 gives

$$\frac{a'}{(1-a)} = \frac{(\sigma C_L)}{4\lambda_r \sin\varphi}\left[1-(C_D/C_L)\cot\varphi\right] \tag{63}$$

By rearranging the equation 63 using equation 50

$$\frac{a'}{(1+a')} = \frac{(\sigma C_L)}{4\cos\varphi}\left[1-(C_D/C_L)\cot\varphi\right] \tag{64}$$

can be obtained. In order to calculation of induction factors *a* and *a'*, C_D can be set to zero for the purpose of determining induction factors independently from airfoil characteristics, so equations 62, 63 and 64 can be rewritten as equation 65, 66, and 67 respectively.

$$\frac{a}{(1-a)} = (\sigma C_L)\frac{\cos\varphi}{4\sin^2\varphi} \tag{65}$$

$$\frac{a'}{(1-a)} = \frac{(\sigma C_L)}{4\lambda_r \sin\varphi} \tag{66}$$

$$\frac{a'}{(1+a')} = \frac{(\sigma C_L)}{4\cos\varphi} \tag{67}$$

Finally, by using the equations 65, 66, and 67 the following useful relationships can be obtained.

$$a = \frac{1}{\left[1+[4\sin^2\varphi/(\sigma C_L)\cos\varphi]\right]} \tag{68}$$

$$a' = \frac{1}{\left[[4\cos\varphi/(\sigma C_L)]-1\right]} \tag{69}$$

$$a/a' = \lambda_r/\tan\varphi \tag{70}$$

$$C_L = \frac{4\sin\varphi}{\sigma}\frac{(\cos\varphi-\lambda_r\sin\varphi)}{(\sin\varphi+\lambda_r\cos\varphi)} \tag{71}$$

The total power from the rotor can be found using

$$P = \int_{r_h}^{R} dP = \int_{r_h}^{R} \Omega dQ \tag{72}$$

and rewriting the equation 18 gives

$$C_p = \frac{P}{1/2\rho U_\infty^3 A} = \frac{\int_{r_h}^{R}\Omega dQ}{1/2\rho U_\infty^3 \pi R^2}$$

Using the equations 60, 65 and 70 the power coefficient formula can be rearranged as

$$C_p = \frac{8}{\lambda^2}\int_{\lambda_h}^{\lambda}\lambda_r^3 a'(1 \quad a)\left[1 \quad (C_D/C_L)\cot\varphi\right]d\lambda_r \tag{73}$$

At the tip of the turbine blade losses are introduced. These can be accounted for in BEM theory by means of a correction factor, f which varies from 0 to 1 and characterizes the reduction in forces along the blade. An approximate method of estimating the effect of tip losses has been given by L. Prandtl and the expression obtained by Prandtl for tip-loss factor is given by the following equation [1]

$$f = \frac{2}{\pi}cos^{-1}\left\{exp\left[\frac{-(B/2)\left[1-(\frac{r}{R})\right]}{\left(\frac{r}{R}\right)sin\varphi}\right]\right\} \tag{74}$$

The application of this equation for the losses at the blade tips is to provide an approximate correction to the system of equations for predicting rotor performance and blade design. Carrying the tip-loss factor through the calculations, the changes will be as following:

$$dQ = 4f\pi\rho U_\infty \Omega a'(1-a)r^3 dr \tag{75}$$

$$dT = 4f\pi\rho U_\infty^2 a(1-a)r dr \tag{76}$$

$$\frac{a'}{1-a} = \frac{\sigma C_L}{4f\lambda_{r\,sin}\varphi} \tag{78}$$

$$\frac{a'}{1-a'} = \frac{\sigma C_L}{4fcos\varphi} \tag{79}$$

$$C_L = \frac{4fsin\varphi}{\sigma}\frac{(cos\varphi-\lambda_{rsin\varphi})}{(sin\varphi+\lambda_{rcos\varphi})} \tag{80}$$

$$a = \frac{1}{1+\left[\frac{4fsin^2\varphi}{(\sigma C_L)cos\varphi}\right]} \tag{81}$$

$$a' = \frac{1}{\left[\frac{4f\cos\varphi}{(\sigma C_L)} - 1\right]} \tag{82}$$

$$C_P = \frac{8}{\lambda^2}\int_{\lambda_h}^{\lambda} f\lambda_r{}^3 a'(1-a)\left[1 - \frac{C_D}{C_L}tan\beta\right]d\lambda_r \tag{83}$$

As a result, for a selected airfoil type and for a specified tip-speed ratio and blade length (i.e. rotor radius), the blade shape can be designed for optimum rotor and using the geometric parameters determined the aerodynamic performance of the rotor can be analyzed.

3. Blade Design Procedure

The aerodynamic design of optimum rotor blades from a known airfoil type means determining the geometric parameters such as chord length distribution and twist distribution along the blade length for a certain tip-speed ratio at which the power coefficient of the rotor is maximum. For this reason firstly the change of the power coefficient of the rotor with respect to tip-speed ratio should be figured out in order to determine the design tip-speed ratio, λ_d corresponding to which the rotor has a maximum power coefficient. The blade design parameters will then be according to this design tip-speed ratio.

Examining the plots between relative wind angle and local tip-speed ratio for a wide range of glide ratios gives us a unique relationship when the maximum elemental power coefficient is considered. And this relationship can be found to be nearly independent of glide ratio and tip-loss factor. Therefore a general relationship can be obtained between optimum relative wind angle and local tip-speed ratio which will be applicable for any airfoil type.

$$\frac{\partial}{\partial\varphi}\left\{\sin^2\varphi\left(\cos\varphi - \lambda_r\sin\varphi\right)\left(\sin\varphi + \lambda_r\cos\varphi\right)\right\} = 0 \tag{85}$$

Equation 85 reveals after some algebra [2];

$$\varphi_{opt} = \left(2/3\right)\tan^{-1}\left(1/\lambda_r\right) \tag{86}$$

Having found the solution of determining the optimum relative wind angle for a certain local tip-speed ratio, the rest is nothing but to apply the equations from equation 80 to 83, which were derived from the blade-element momentum theory and modified including the tip loss factor, to define the blade shape and to find out the maximum power coefficient for a selected airfoil type.

Dividing the blade length into *N* elements, the local tip-speed ratio for each blade element can then be calculated as

$$\lambda_{r,i} = \lambda\left(r_i/R\right) \tag{87}$$

Then rewriting equation 86 for each blade element gives

$$\varphi_{opt,i} = \left(2/3\right)\tan^{-1}\left(1/\lambda_{r,i}\right) \tag{88}$$

Also the tip loss correction factor for each element can be calculated as

$$f_i = \frac{2}{\pi}cos^{-1}\left\{exp\left[\frac{-(B/2)\left[1-(\frac{r_i}{R})\right]}{\left(\frac{r_i}{R}\right)sin\varphi_{opt,i}}\right]\right\} \tag{89}$$

Chord-length distribution can then be calculated for each blade element by using equation 90 [1]

$$c_i = \frac{8\pi r_i F_i \sin\varphi_{opt,i}}{BC_{L,design}}\frac{(\cos\varphi_{opt,i} - \lambda_{r,i}\sin\varphi_{opt,i})}{(\sin\varphi_{opt,i} + \lambda_{r,i}\cos\varphi_{opt,i})} \tag{90}$$

where $C_{L_{design}}$ is chosen such that the glide ratio is minimum at each blade element.

The twist distribution can easily be determined by using equation 91

$$\theta_i = \varphi_{opt,i} - \alpha_{design} \tag{91}$$

where α_{design} is again the design angle of attack at which $C_{L_{design}}$ is obtained.

Now the parameters such as chord-length and twist distribution along the blade length are known and in this case lift coefficient and angle of attack have to be determined from the known blade geometry parameters. This requires an iterative solution in which for each blade element the axial and angular induction factors are firstly taken as the values which were found for the corresponding designed blade elements and then determined within an acceptable tolerance of the previous guesses of induction factors during iteration.

Applying the design procedure explained a computer program is written to design new blades and to estimate the aerodynamic performance of the existing blades. A detailed flow chart of the program is given in Figure 6.

4. Results

The geometry and configuration of the designed rotor is summarized in Table 1. As it can be seen clearly from Table 1 the rotor employs an NREL S809 airfoil profile at inboard, mid-span and outboard stations of the blades. The S809 profile is also uniquely defined by its coordinates which appear in Table 2 and also shown graphically in Figure 7.

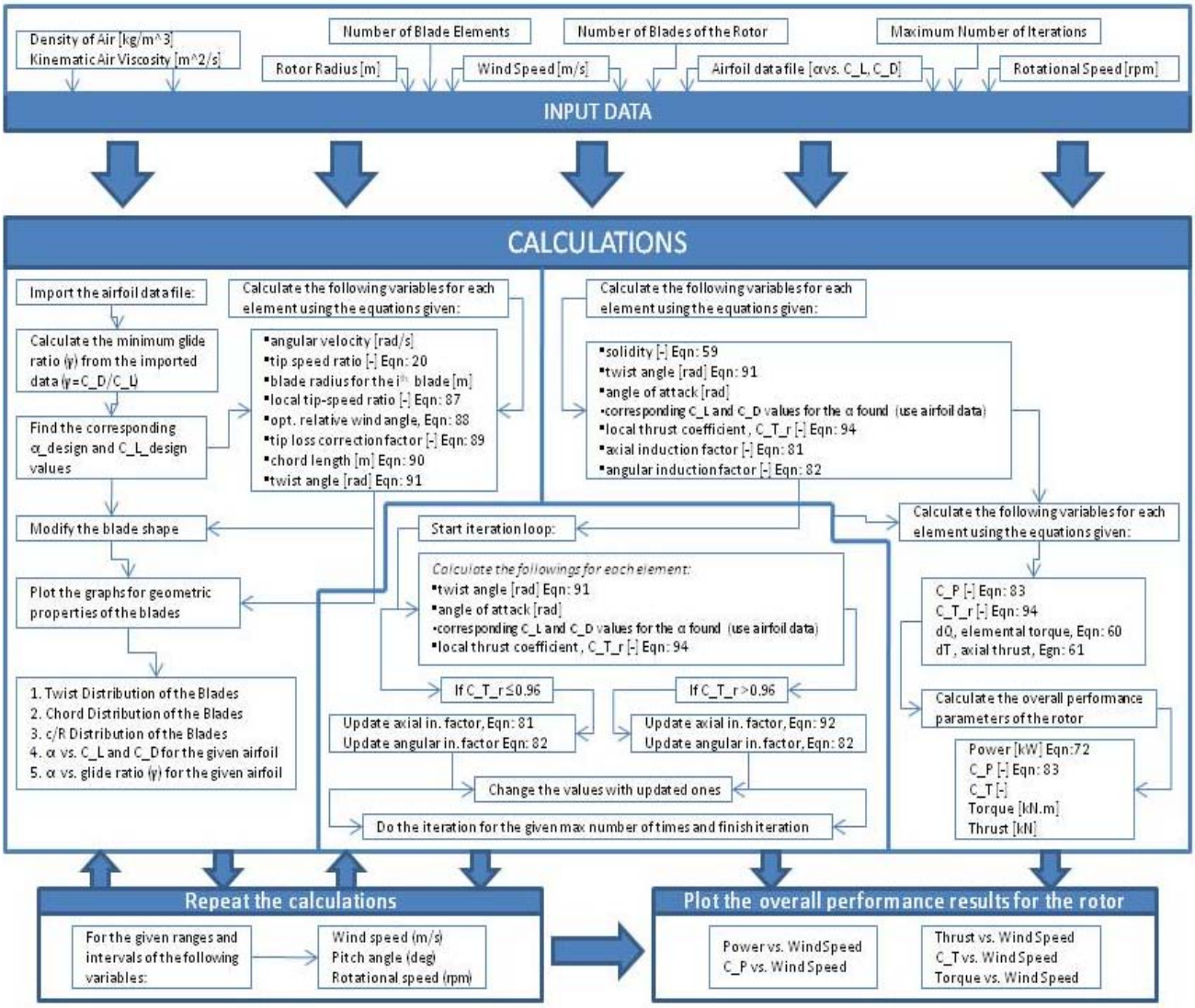

Figure 6. Computer Program Flow Chart

Table 1 Properties of the Designed Blades

Property	Value
Blade Length (m)	8.5451
Hub Radius (m)	0.8915
Tip Radius (m)	9.4366
Total Blade Twist Angle	6.82 deg
Operational Pitch Setting	-1.0 deg
Tested Rotational Speed	70.00 rpm
Blade Coning Angle	7.00 deg
Root (inboard) Airfoil	S809
Mid-span Airfoil	S809
Tip (outboard) Airfoil	S809
Maximum Chord (m)	1.0400
Maximum Chord Station (m)	3.5387
Tip Chord (m)	0.3326
Root Chord (m)	0.7583
Number of Blades	3
Rotor Radius (m)	9.4366
Hub Radius (m)	0.5415
Pre-cone Angle (deg)	6.0
Shaft Tilt Angle (deg)	0.0
Hub Height (m)	34.9154

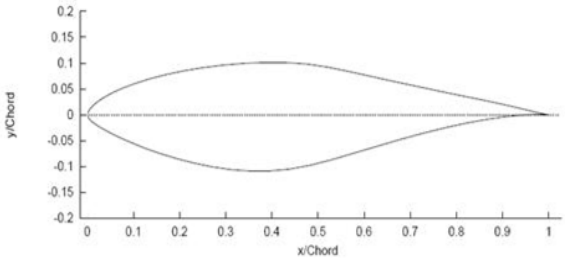

Figure 7. S809 Aerofoil [3]

Table 2 Coordinates of the S809 Airfoil [2]

Upper Surface		Lower Surface	
x/c	y/c	x/c	y/c
0.00037	0.00275	0.0014	-0.00498
0.00575	0.01166	0.00933	-0.01272
0.01626	0.02133	0.02321	-0.02162
0.03158	0.03136	0.04223	-0.03144
0.05147	0.04143	0.06579	-0.04199
0.07568	0.05132	0.09325	-0.05301
0.10390	0.06082	0.12397	-0.06408
0.13580	0.06972	0.15752	-0.07467
0.17103	0.07786	0.19362	-0.08447
0.20920	0.08505	0.23175	-0.09326
0.24987	0.09113	0.27129	-0.10060
0.29259	0.09594	0.31188	-0.10589
0.33689	0.09933	0.35328	-0.10866
0.38223	0.10109	0.39541	-0.10842
0.42809	0.10101	0.43832	-0.10484
0.47384	0.09843	0.48234	-0.09756
0.52005	0.09237	0.52837	-0.08697
0.56801	0.08356	0.57663	-0.07442
0.61747	0.07379	0.62649	-0.06112
0.66718	0.06403	0.67710	-0.04792
0.71606	0.05462	0.72752	-0.03558
0.76314	0.04578	0.77668	-0.02466
0.80756	0.03761	0.82348	-0.01559
0.84854	0.03017	0.86677	-0.00859
0.88537	0.02335	0.90545	-0.00370
0.91763	0.01694	0.93852	-0.00075
0.94523	0.01101	0.96509	0.00054
0.96799	0.00600	0.98446	0.00065
0.98528	0.00245	0.99612	0.00024
0.99623	0.00054	1	0
1	0		

Lift and Drag coefficients for S809 aerofoil are shown in Figure 8. This plot shows that for low values of angle of attack the aerofoil successfully produces a large amount of lift with little drag. At around α = 16 a phenomenon known as stall occurs where there is a massive increase in drag and a sharp reduction in lift.

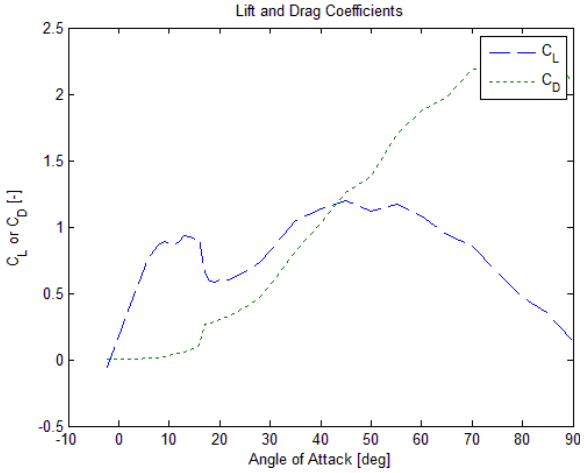

Figure 8. Lift and Drag Coefficients for S809 Aerofoil

Also the variation of glide ratio of S809 airfoil with different angle of attacks is illustrated in Figure 9. As it is stated before, there is clearly a significant reduction in maximum achievable power as the airfoil drag increases. Since it clearly benefits the blade designer to use or design airfoils with low glide ratio, α and C_L values which corresponds to the minimum glide ratio is chosen as α_{design} and $C_{L,design}$ using the airfoil data file.

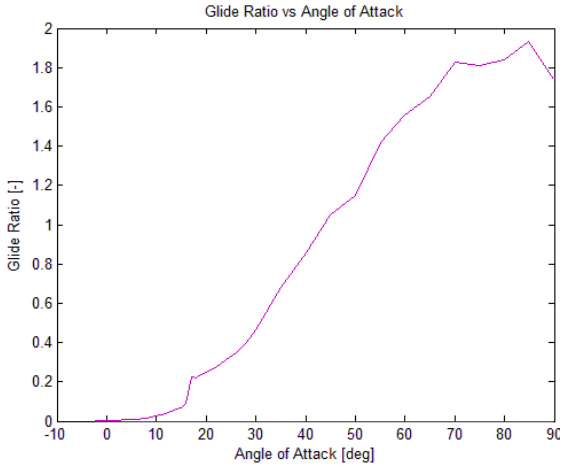

Figure 9. Glide Ratio vs. α for S809 Aerofoil

Table 3 contains the local twist distribution and chord distribution schedules for the designed rotor blades. Also the twist and chord distribution schedules are presented graphically in Figure 10 and 11 respectively.

Table 3 Geometric properties of the designed blades

r/R	Station [m]	twist [deg]	chord [m]	c/R
0.100	0.892	22.264	0.758	0.080
0.156	1.180	14.510	0.802	0.085
0.213	1.769	11.103	0.888	0.094
0.269	2.359	9.663	0.962	0.102
0.325	2.949	7.920	1.012	0.107
0.381	3.539	6.474	1.040	0.110
0.438	4.129	5.451	1.028	0.109
0.494	4.718	4.697	0.956	0.101
0.550	5.308	4.121	0.882	0.094
0.606	5.898	3.668	0.809	0.086
0.663	6.488	3.302	0.750	0.080
0.719	7.077	3.001	0.682	0.072
0.775	7.667	2.750	0.619	0.066
0.831	8.257	2.538	0.535	0.057
0.888	8.847	2.356	0.458	0.049
1.000	9.437	2.199	0.333	0.035

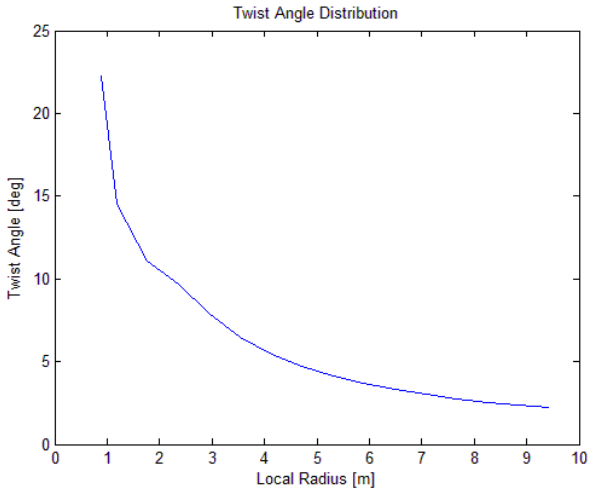

Figure 10. Twist Angle Distribution of the Designed Blades

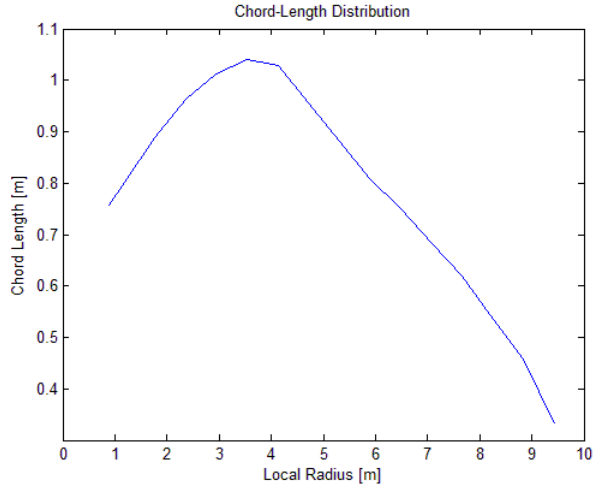

Figure 11. Chord-Length Distribution of the Designed Blades

The change of the performance parameters of the designed rotor such as power C_P, bending moment, thrust with respect to the wind speed is given in Figure 12, 13, 14 and 15 respectively. As it can be seen from the figures the analysis has been repeated for different values of the pitch angle at the rotational speed of 70 rpm.

Also the 3-D views of the designed blades and rotor are given in the Figure 16, 17, 18 and Figure 19 respectively. The dimensions and the geometric properties with the configuration of the rotor are given in Table 1 and Table 3.

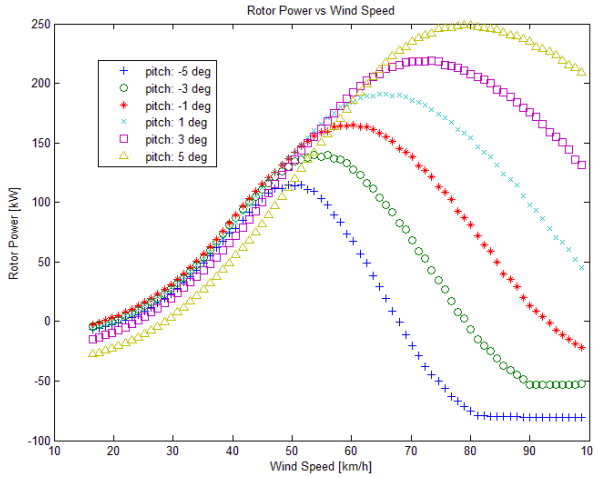

Figure 12. Power vs. Wind Speed for the Designed Rotor

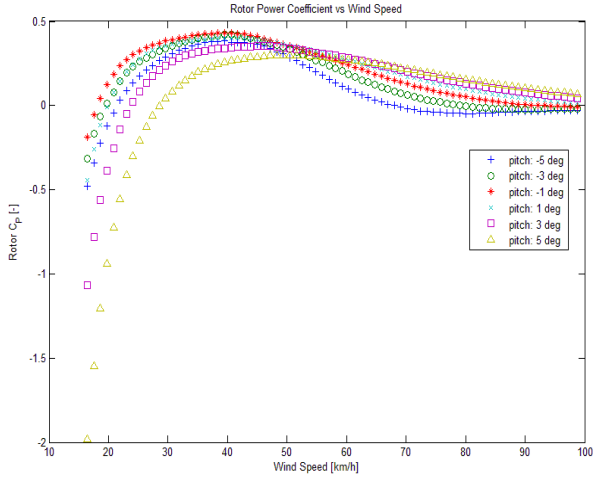

Figure 13. C_P vs. Wind Speed for the Designed Rotor

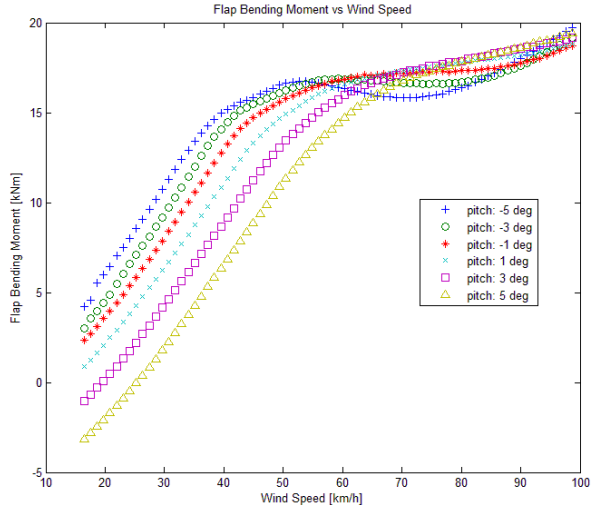

Figure 14. Bending Moment vs. Wind Speed for the Designed Rotor

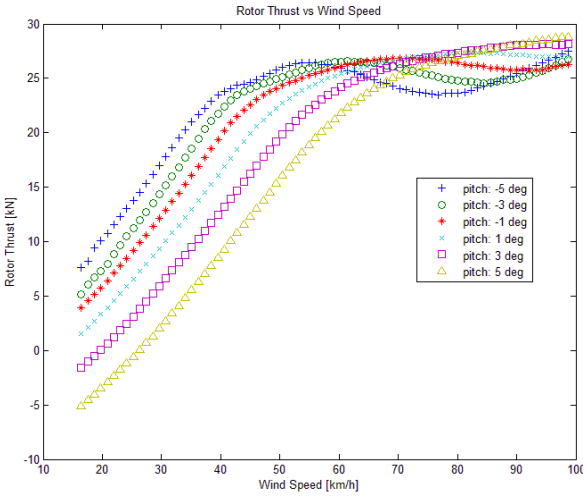

Figure 15. Thrust vs. Wind Speed for the Designed Rotor

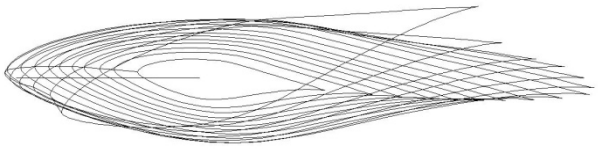

Figure 16. Views of Blade Elements from Root towards Tip

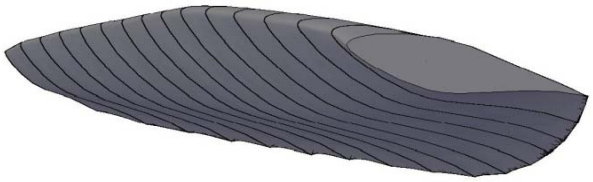

Figure 17. 3D View of the Designed Blade

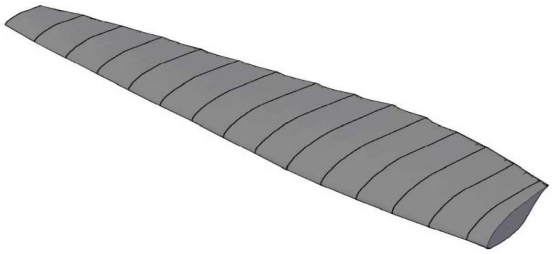

Figure 18. 3D View of the Designed Blade

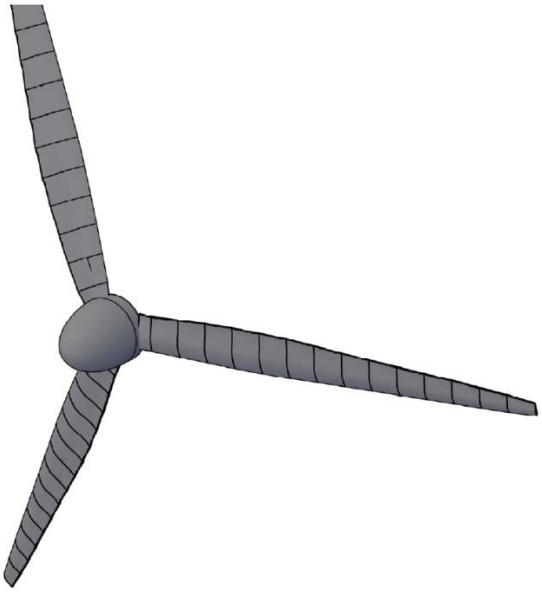

Figure 19. 3D View of the Designed Rotor

REFERENCES

[1] Burton, T. and Sharpe, D., Wind Energy Handbook. John Wiley & Sons Ltd, Chichester, 2006.

[2] Hau, E., Wind Turbines: Fundamentals, Technologies, Application, Economics. Krailling, Springer, 2006.

[3] Bertagnolio, F., Niels Sorensen, N., Johansen, J., Fuglsang, P., Wind Turbine Airfoil Catalogue. Riso National Laboratory, Roskilde, 2001.

[4] Mathews, J. H. and Fink, K. D., Numerical Methods Using MATLAB. Prentice Hall, Upper Saddle River, 1999.

[5] Hunt, B. R. and Lipsman, R. L., A Guide to MATLAB: For Beginners and Experienced Users. Cambridge University Press, New York, 2001.

[6] Wilson, R. E., Lissaman, P. B. S., Walker, S. N., “Aerodynamic Performance of Wind Turbines”. Energy Research and Development Administration, 224, 1976.